Microsyst Technol (2007) 13:1353–1358
DOI 10.1007/s00542-006-0368-8

TECHNICAL PAPER

Deposition of Si-DLC film and its microstructural, tribological and corrosion properties

Junho Choi · Masahiro Kawaguchi · Takahisa Kato · Masami Ikeyama

Received: 27 June 2006 / Accepted: 30 November 2006 / Published online: 5 January 2007

Abstract Silicon-incorporated diamond-like carbon (Si-DLC) films were deposited using a bipolar-type plasma based ion implantation and deposition technique, and the effects of Si-incorporation on the microstructural, tribological, anti-corrosion and lubricant bonding properties of the Si-DLC films were investigated. The analysis of Raman spectroscopy exhibited that the sp^3 bonds in the DLC film increase due to Si addition. XPS analysis revealed that a thick oxide layer exists on the Si-DLC film surfaces. These explain the high lubricant bonding properties of the Si-DLC films compared to that of the Si-free DLC films. The silicon oxide layer on the Si-DLC film and the transferred silicon oxide layer on the steel ball prevents from the metal/DLC contact between the Si-DLC film and steel ball when sliding, which results in a low friction. Incorporation of Si in DLC films led to significant improvements in the corrosion resistance due to low internal stress and thick insulating oxide layer.

J. Choi (✉) · M. Ikeyama
National Institute of Advanced Industrial Science and Technology (AIST), 2266-98 Anagahora, Shimoshidami, Moriyama-ku, Nagoya, Aichi 463-8560, Japan
e-mail: junho.choi@aist.go.jp

M. Kawaguchi
Tokyo Metropolitan Industrial Technology Research Institute (TIRI), 3-13-10 Nishigaoka, Kita-ku, Tokyo 115-8586, Japan

T. Kato
The University of Tokyo, 7-3-1 Hongo, Tokyo 113-8656, Japan

1 Introduction

Silicon-incorporated diamond-like carbon (Si-DLC) films have excellent properties such as low friction, high durability, and stability against humidity and temperature (Oguri and Arai 1991). Moreover, Si addition improves surface roughness and adhesion strength. These superior properties of the Si-DLC films make them as candidates for a protective coating in micro and nano-system such as microelectromechanical systems (MEMS) and magnetic disk drives. In the case of magnetic disk drives, since the thickness of protective DLC coatings decreases to several nanometers to achieve much higher recording density, DLC coatings which have better tribological and anti-corrosion properties are required (Bhushan 1999).

Ultrathin organic films such as perfluoropolyethers are employed in MEMS (Lee et al. 2000) and magnetic disk drives (Homola 1996) to protect the system from stiction and corrosion. The strong bonding between solid surface and organic molecules is required to reduce these problems. The lubricant bonding toward the solid surfaces is related to the structure and chemistry of the solid surface, since the end groups of organic molecules are adsorbed to adsorption sites on the solid surfaces (Yanagisawa 1994). To obtain high molecular bonding, it is necessary to increase the number of adsorption sites on the solid surface, we consider, which can be achieved by modifying the solid surface. In the case of protective DLC coatings, some elements such as silicon can be added in the carbon network for this. In this article, we review various properties of the Si-DLC films and explain the low friction and high molecular bonding mechanism and good corrosion performance of the Si-DLC films.

2 Deposition of Si-DLC films

The Si-DLC films were deposited using a bipolar-type plasma based ion implantation and deposition (PBII&D) (Miyagawa 2002). The schematic diagram of the PBII is shown in Fig. 1. The glow discharge plasma is formed around the target surface by applying a positive pulse voltage directly to the target, and the plasma is omnidirectionally implanted into (or deposited on) the target surface by a subsequent negative high pulse voltage. The PBII processing with bipolar pulses provides improved adhesion strength between the DLC film and the target. A gas mixture of tetramethylsilane [TMS, $Si(CH_3)_4$] and toluene was used for the deposition of the Si-DLC films. The ratio of TMS and toluene in the gas mixture were change to obtain the Si-DLC film with various Si contents, whereas the deposition pressure was kept constant. The deposition conditions of the Si-DLC films are shown in Table 1. The composition and microstructure of the deposited Si-DLC films were measured and analyzed using X-ray photoelectron spectroscopy (XPS) and Raman spectroscopy. The film thickness was measured with a microstylus profilometer.

Table 1 Deposition conditions for the Si-DLC films

Precursor gas	TMS/toluene mixture
Deposition pressure	0.1 Pa
Positive pulse	(+) 2.0 kV
Negative pulse	(–) 5.0 kV
Pulse frequency	4 kHz
Pulse duration	5 μs

3 Microstructure of Si-DLC Films

Figure 2 shows (1) Raman spectra of the Si-DLC films, and (2) I_D/I_G ratio and G-peak position determined from the Raman spectra. The G- and D-peak positions of the Si-free DLC film and the change of the G-peak positions for the Si-DLC films are indicated using arrows. The Si-free DLC film shows a typical diamond-like structure with peaks centered at 1,539 (G band) and 1,373 cm^{-1} (D band). With the increasing Si content, the G-peak becomes more pronounced relative to the D-peak, and the peak for 29 at. % Si-DLC film can be fitted by a single Gaussian. The G-peak position is shifted to a low wavenumber from 1,539 to 1,461 cm^{-1}, and the intensity ratio, I_D/I_G, decreases from 0.81 to 0.15 with the increasing Si content up to 29 at.%. Incorporation of more Si atoms into the carbon network reduces the phonon vibration frequency because the Si atom is heavier than the C atom, causing a

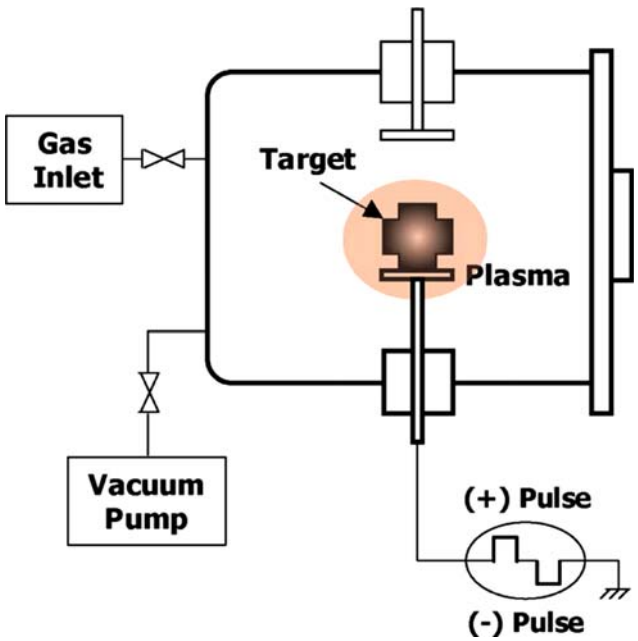

Fig. 1 Schematic diagram of PBII&D used for the deposition of Si-DLC films

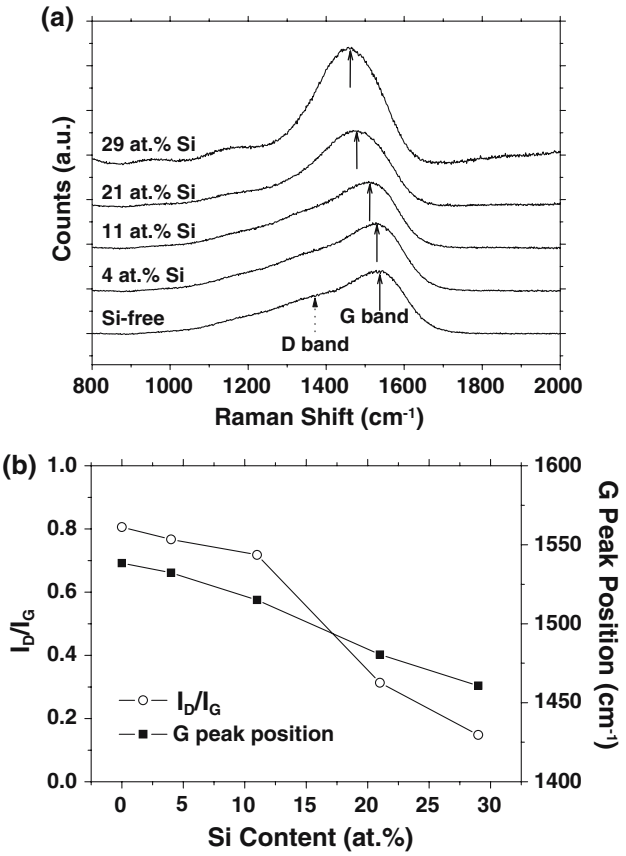

Fig. 2 **a** Raman spectra of the Si-DLC films, **b** I_D/I_G ratio and G-peak position determined from the Raman spectra

G-peak shift to low wavenumbers (Abbas et al. 2005a, b). The D-peak is due to six-folder (sp^2) rings (Robertson 2002). The Si-incorporation causes an opening up of the sp^2 rings and decreases of the sp^2 cluster size because the Si atoms can not form the π bonds (Abbas et al. 2005, b), in a result, I_D/I_G decreases with the increasing Si content. These behaviors indicate that the sp^3 bonds increase with the increasing Si content in the Si-DLC film.

Figure 3 shows the depth profiles of oxygen contents in the Si-free and Si-DLC film surfaces. The oxygen contents were measured using XPS before and after Ar^+ ion sputtering. The sputter rate was about 0.05 nm/s. It is observed that the oxygen content in the DLC film surface increases due to Si addition. Furthermore, the oxygen content on the Si-DLC film surface increases with the increasing Si content. The oxygen content in the Si-free DLC film surface becomes negligible after Ar^+ ion sputtering for 20 s, which indicates that the oxide thickness on the Si-free DLC surface is about 1 nm. On the other hand, the Si-DLC film has a thicker oxide layer compared to that of the Si-free DLC film.

Recently, the bonding characteristics of perfluoropolyether (PFPE, Fomblin ZDOL4000) molecules, having a hydroxyl end group, regarding to the Si-DLC films were investigated using conventional dip coating (Choi et al. 2006). It was found that Si incorporation enhances the molecular bonding of PFPE lubricant on the DLC film surfaces, and the bonding increases with the increasing Si content in the DLC film. These results are attributed to structural and chemical modifications of the DLC surfaces due to Si incorporation into the carbon network. The molecular bonding of lubricant is related to the kinds of functional end groups of lubricants, the kinds of solid surfaces (i.e., the number of adsorption sites) and the contamination of solid surfaces as illustrated in Fig. 4. Yanagisawa reported that oxygen-containing functional groups and dangling bonds are effective adsorption sites for the PFPE molecules having hydroxyl end groups (Yanagisawa 1994). Kasai described the sputtered carbon films as stacks of spheroidal granules of several nanometers in diameter. Each individual granule would have either the sp^2 (graphitic) bonding scheme or sp^3 (diamond-like) bonding scheme, and the large number of dangling bonds are generated and trapped only within the tight three dimensional networks of diamond-like granules (Kasai 2000). The Si addition to the DLC surface increases the sp^3 bonds (i.e., the number of dangling bonds) and the oxygen groups in the carbon surface as exhibited from Raman (Fig. 2) and XPS (Fig. 3) results, which explains the good bonding properties of PFPE molecules toward the Si-DLC film.

4 Friction properties of Si-DLC films

Figure 5 shows the internal stress and friction coefficient of the Si-DLC films deposited on Si substrates. The internal stress? was calculated using Stoney equation by measuring the curvature radii of the DLC-coated silicon substrates with a microstylus profilometer. The internal stress of the DLC films deposited by PBII exhibits a very low value compared to that of DLC film deposited by conventional PECVD process (Wu and Hon 1997). The internal stress further decreases below 0.2 GPa due to the Si addition. Wu and Hon reported that the low internal stress of the

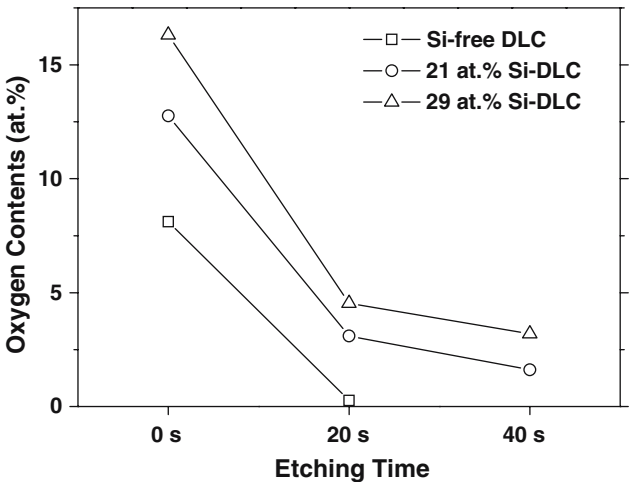

Fig. 3 The depth profiles of oxygen contents in the Si-free and Si-DLC film surfaces measured with XPS

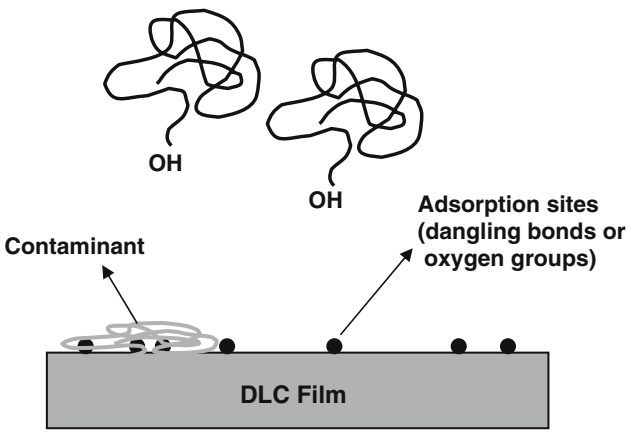

Fig. 4 Schematic diagram of lubricant bonding on the DLC film surface

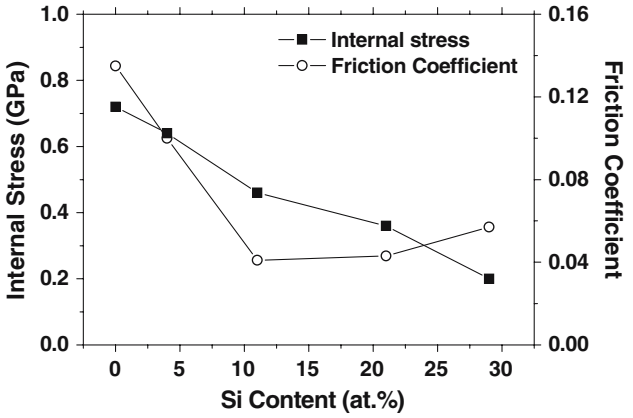

Fig. 5 The internal stress and friction coefficient of the Si-DLC films

Si-DLC films is due to the polymer-like structure of the films, i.e., high hydrogen content and low hardness (Wu and Hon 1997).

The friction coefficients of the DLC films deposited on steel substrates (SKD61) were measured by a ball-on-flat type reciprocal friction tester in ambient air. The applied load, the reciprocal sliding distance, the sliding speed, and diameter of the steel balls (SUJ2) were 0.98 N, 8 mm, 0.5 Hz, and 3 mm, respectively. The film thickness of the Si-free DLC and Si-DLC films varied from 1 to 2 μm regarding to the deposition ratio. The deposition ratio decreased with increasing the TMS volume fraction in the gas mixture. The friction coefficient of the DLC film decreases to a very low value of 0.04 due to Si-incorporation. Figure 6 shows (1) SEM, (2) Si mapping and (3) O mapping images of steel ball surface slid against 29 at.% Si-DLC film. The Si and O mapping images were obtained by electron probe microanalysis (EPMA). The bright regions of Fig. 6b and c are Si-rich and O-rich regions, respectively, and the dark regions of Fig. 6b and c are Fe-rich regions originating from the steel ball. As can be seen in Fig. 6, the distribution of Si on worn ball surface corresponds to that of O, which indicates that the silicon oxide is transferred on the steel ball surface after sliding. The low friction of the Si-DLC films is related to the formation of silicon-rich oxide debris and transferred silicon oxide layers on the steel ball surfaces. The silicon oxide layers on the Si-DLC film (see Fig. 3) and steel ball prevent from the metal/DLC contact between the Si-DLC film and steel ball when sliding, which results in a low friction. In the case of the Si-free DLC film, the steel ball surface is seriously damaged as shown in Fig. 7, which results in a high friction coefficient. Another possible explanation on the low friction properties of the Si-DLC films is the

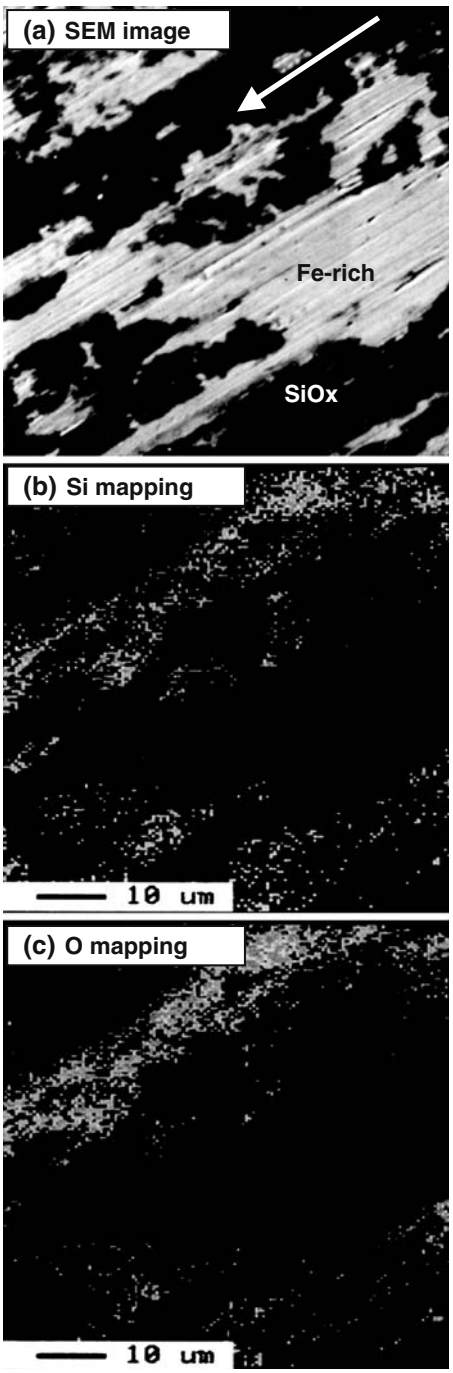

Fig. 6 **a** SEM, **b** Si mapping, **c** O mapping images of steel ball surface after sliding against 29 at.% Si-DLC film. The *bright* regions of (**b**) and (**c**) are Si-rich and O-rich regions, respectively. The *dark* regions of (**b**) and (**c**) are Fe-rich regions originating from the steel ball

effect of water lubrication. The adsorbed water molecules on SiOH groups existing on the Si-DLC film surfaces reduce shear strength between the Si-DLC film and steel ball (Patton et al. 2000).

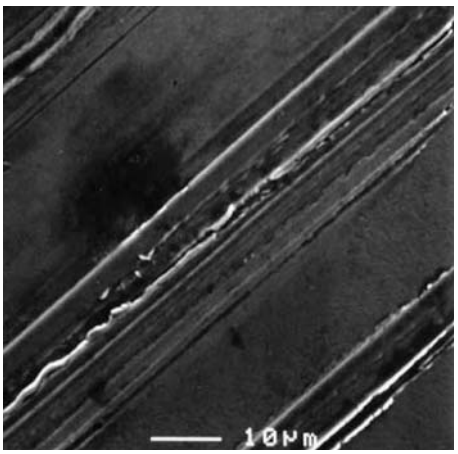

Fig. 7 SEM image of the steel ball surface after sliding against Si-free DLC film

5 Anti-corrosion properties of Si-DLC films

Potentiodynamic polarization experiments were conducted to evaluate the corrosion performance of the Si-DLC films in aqueous 0.05 M NaCl solution. The Si-DLC films were deposited on glass plates coated with magnesium alloy films. The film thickness of the DLC films were adjusted to 800 nm from the deposition rates. The magnesium films were deposited using an ion beam sputter with a magnesium alloy target (AZ31, Mg–3%Al-1%Zn). A Pt sheet and a saturated calomel electrode (SCE) were used as counter and reference electrodes, respectively. For comparison purpose, a result of substrate (i.e., glass plate coated with magnesium alloy film) is also included.

Figure 8a is the potentiodynamic curves which are usually obtained from the potentiodynamic polarization experiments. The curve is the total current, that is, the sum of the anodic and cathodic currents. Figure 8b is obtained by converting the current density (the vertical axis of Fig. 8a) as the logarithm of absolute current density. The sharp point in the curve is the point where the current changes signs as the reaction changes from cathodic to anodic (or from anodic to cathodic). The corrosion currents and corrosion potentials are obtained from Fig. 8b by Tafel analysis (Stippich et al. 1998), and the values are shown in Table 2. The corrosion potential of the Si-free DLC coated sample was shifted 0.6 V to positive direction compared to the substrate. Moreover, the corrosion potential of the Si-DLC coated sample was shifted to more positive value compared to that of the Si-free DLC coated sample. It indicates that the corrosion protection performance of the Si-DLC film is superior to that of the Si-free DLC film. The corrosion current density of the Si-DLC coated sample is three orders of

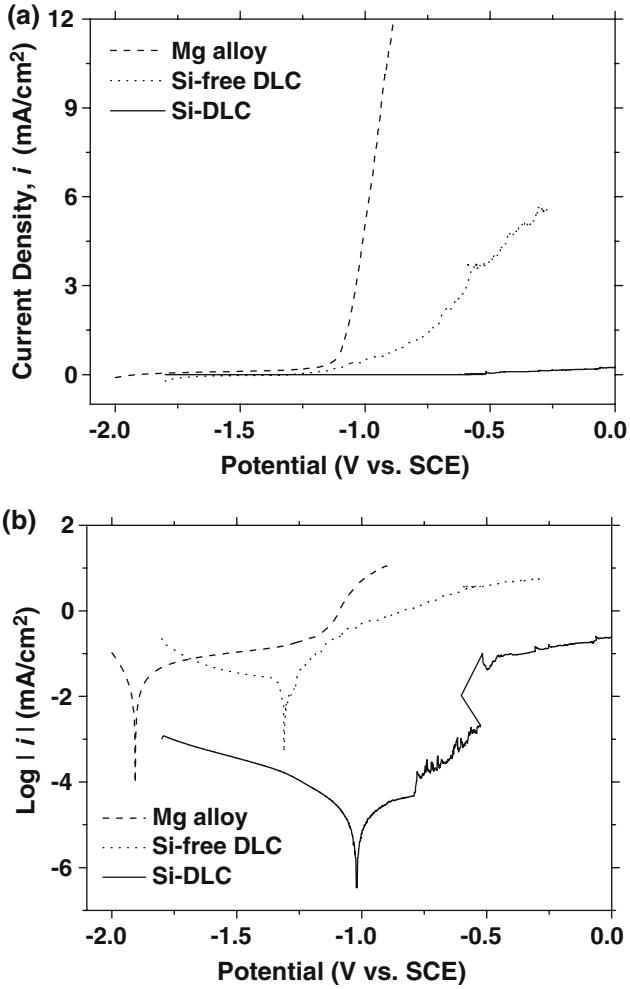

Fig. 8 Polarization curves for the Si-free DLC and Si-DLC films deposited on magnesium alloy films

magnitude lower than that of the Si-free DLC coated sample, whereas the corrosion current of the Si-free DLC coated sample is comparable to that of uncoated substrate. The lower this value, the better the corrosion protection property, because the corrosion current is directly related to the corrosion rate. XPS measurements exhibited that silicon oxide layer exists on the Si-DLC surface. The insulating silicon oxide layer results in good anti-corrosion properties of the Si-DLC films (Fig. 3). Another reason is the very low internal stress of the Si-DLC films as shown in Fig. 5. The high

Table 2 Corrosion potentials and corrosion currents

Samples	Corrosion potential (V)	Corrosion current (mA)
Magnesium alloy	–1.9	5.2×10^{-2}
Si-free DLC coating	–1.3	2.2×10^{-2}
Si-DLC coating	–1.0	2.1×10^{-5}

internal stress causes the surface cracking and, consequently, poor anti-corrosion properties.

6 Conclusion

The various properties of the Si-DLC films—microstructural, tribological, anti-corrosion and PFPE bonding properties - were investigated. The results are as follows:

1. The analysis of Raman spectroscopy indicated that the sp^3 bonds in the DLC film increase with the increasing Si content. Also, the Si-DLC films have high oxygen contents on the surfaces. These explain the high molecular bonding properties of PFPE lubricant toward the Si-DLC film surface due to increased adsorption sites.
2. The silicon oxide layer on the Si-DLC film and the transferred silicon oxide layer on the steel ball prevent from the metal/DLC contact between the Si-DLC film and steel ball when sliding, which results in a low friction.
3. The Si-DLC film shows a low internal stress, and Si incorporation in the DLC film creates a thick insulating oxide layer on the film. These lead to significant improvements in the corrosion properties of the DLC film.

References

Abbas GA et al (2005a) Hydrogen softening and optical transparency in Si-incorporated hydrogenated amorphous carbon films. J Appl Phys 98:103505-1–103505-6

Abbas GA et al (2005b) The improvement in gas barrier performance and optical transparency of DLC-coated polymer by silicon incorporation. Thin Solid Films 482:201–206

Bhushan B (1999) Chemical, mechanical and tribological characterization of ultrathin and hard amorphous carbon coatings as thin as 3.5 nm: recent developments. Diamond Relat Mater 8:1985–2015

Choi J et al (2006) Deposition of perfluoropolyether lubricant films on Si-incorporated diamond-like carbon surfaces. J Appl Phys 97:08N109-1–08N109-3

Homola AM (1996) Lubrication issues in magnetic disk storage devices. IEEE Trans Magn 32:1812–1818

Kasai PH (2000) Carbon overcoat: structure and bonding of Z-DOL. Proc Int Tribol Conf, Tribochemistry Tsukuba, pp 63–68

Lee KK et al (2000) Chemical, optical and tribological characterization of perfluoropolymer films as an anti-stiction layer in micromirror arrays. Thin Solid Films 377–378:727–732

Miyagawa S et al (2002) Deposition of diamond-like carbon films using plasma based ion implantation with bipolar pulses. Surf Coat Technol 156:322–327

Oguri K, Arai T (1991) Tribological properties and characterization of diamond-like carbon coatings with silicon prepared by plasma-assisted chemical deposition. Surf Coat Technol 47:710–721

Patton ST et al (2000) Effect of surface chemistry on the tribological performance of a MEMS electrostatic lateral output motor. Tribol Lett 9:199–209

Robertson J (2002) Diamond-like amorphous carbon. Mater Sci Eng R 37:129–281

Stippich F et al (1998) Enhanced corrosion protection of magnesium oxide coatings on magnesium deposited by ion beam-assisted evaporation. Surf Coat Technol 103–104:29–35

Wu W, Hon M (1997) The structure and residual stress in Si containing diamond-like carbon coating. Thin Solid Film 307:1–5

Yanagisawa M (1994) Adsorption on perfluoro-polyethers on carbon surfaces. STLE SP-36:25–32